TU/e EINDHOVEN UNIVERSITY OF TECHNOLOGY

Substrate-biasing during plasma-assisted atomic layer deposition to tailor metal-oxide thin film growth

Citation for published version (APA):
Profijt, H. B., Sanden, van de, M. C. M., & Kessels, W. M. M. (2013). Substrate-biasing during plasma-assisted atomic layer deposition to tailor metal-oxide thin film growth. *Journal of Vacuum Science and Technology A: Vacuum, Surfaces, and Films*, *31*, 01A106-1/10. https://doi.org/10.1116/1.4756906

DOI:
10.1116/1.4756906

Document status and date:
Published: 01/01/2013

Document Version:
Publisher's PDF, also known as Version of Record (includes final page, issue and volume numbers)

Please check the document version of this publication:

• A submitted manuscript is the version of the article upon submission and before peer-review. There can be important differences between the submitted version and the official published version of record. People interested in the research are advised to contact the author for the final version of the publication, or visit the DOI to the publisher's website.
• The final author version and the galley proof are versions of the publication after peer review.
• The final published version features the final layout of the paper including the volume, issue and page numbers.

Link to publication

General rights
Copyright and moral rights for the publications made accessible in the public portal are retained by the authors and/or other copyright owners and it is a condition of accessing publications that users recognise and abide by the legal requirements associated with these rights.

• Users may download and print one copy of any publication from the public portal for the purpose of private study or research.
• You may not further distribute the material or use it for any profit-making activity or commercial gain
• You may freely distribute the URL identifying the publication in the public portal.

If the publication is distributed under the terms of Article 25fa of the Dutch Copyright Act, indicated by the "Taverne" license above, please follow below link for the End User Agreement:

www.tue.nl/taverne

Take down policy
If you believe that this document breaches copyright please contact us at:

openaccess@tue.nl

providing details and we will investigate your claim.

Download date: 25. Aug. 2022

Substrate-biasing during plasma-assisted atomic layer deposition to tailor metal-oxide thin film growth

H. B. Profijt, M. C. M. van de Sanden, and W. M. M. Kessels[a)]
Department of Applied Physics, Eindhoven University of Technology, P.O. Box 513, 5600 MB Eindhoven, The Netherlands

(Received 8 August 2012; accepted 18 September 2012; published 4 October 2012)

Two substrate-biasing techniques, i.e., substrate-tuned biasing and RF biasing, have been implemented in a remote plasma configuration, enabling control of the ion energy during plasma-assisted atomic layer deposition (ALD). With both techniques, substrate bias voltages up to −200 V have been reached, which allowed for ion energies up to 272 eV. Besides the bias voltage, the ion energy and the ion flux, also the electron temperature, the electron density, and the optical emission of the plasma have been measured. The effects of substrate biasing during plasma-assisted ALD have been investigated for Al_2O_3, Co_3O_4, and TiO_2 thin films. The growth per cycle, the mass density, and the crystallinity have been investigated, and it was found that these process and material properties can be tailored using substrate biasing. Additionally, the residual stress in substrates coated with Al_2O_3 films varied with the substrate bias voltage. The results reported in this article demonstrate that substrate biasing is a promising technique to tailor the material properties of thin films synthesized by plasma-assisted ALD.
© *2013 American Vacuum Society*. [http://dx.doi.org/10.1116/1.4756906]

I. INTRODUCTION

For certain materials and processes, plasma-assisted atomic layer deposition (ALD) allows for an increased level of freedom in processing conditions and material properties. This is facilitated by the reactive species generated in the plasma and present during the deposition process.[1] These species include radicals, electrons, ions, and photons. The extent to which ions can contribute to the ALD process depends on their energy and flux, parameters that can be controlled by many variables including the plasma gas mixture, the gas pressure, the power coupled in to the plasma, the reactor design, the type of plasma source, and the possible presence of substrate biasing.[1–5]

A number of ion-induced effects have been reported, which may also be relevant for plasma-assisted ALD. One of those is adatom migration, which is known to enhance (initial) film nucleation.[6–8] In the case of ALD, nucleation delays may be reduced, and for polycrystalline films, the crystallinity may be enhanced when adatom migration is promoted. Another ion-induced effect is the desorption of surface species,[7] which can possibly assist ligand-desorption during the second half-cycle of an ALD process. Subplantation (i.e., subsurface-implantation) is another process which may take place, during which the top few monolayers of the ALD film or the substrate are modified by shallow implantation effects.[6,7] Consequently, the physical or chemical properties of thin films can be affected, which potentially results in a higher film density or the promotion of crystallization of the films at relatively low deposition temperatures.[7,8] It has furthermore been reported that energetic ions can induce or enhance compressive film stress by the subplantation of energetic ions.[6,9]

In our recent work, we discussed that during remote-plasma ALD, the energies and fluxes of the ions are typically sufficiently high to play a role during the deposition process, e.g., by stimulating ligand-removal and enhancing adatom migration.[2] In a follow-up paper, the successful implementation of substrate biasing in a remote plasma ALD reactor was reported, which allows for controlling of the average ion energy.[10] Accordingly, it was demonstrated that the crystalline phase of TiO_2 films can be tailored from anatase to rutile by varying the substrate bias voltage from 0 to −200 V. Also the concentration of hydroxyl groups in the TiO_2 films was shown to be affected by substrate biasing. Moreover, in an independent study, the effects of higher radical and ion fluxes were shown by Kim *et al*. for a plasma-assisted ALD reactor with a remote capacitively coupled plasma.[11] In this reactor configuration, the plasma was generated between an electrode and a grid with a pulsed negative DC voltage applied to it. The substrate was placed downstream with respect to the grid. The authors reported on HfO_2 dielectric films with a decreased equivalent oxide thickness and an increased dielectric breakdown voltage.

Notwithstanding the fact that substrate biasing has been used for many years during plasma-processing techniques such as plasma-enhanced chemical vapor deposition (CVD) and plasma-enhanced physical vapor deposition (PVD), the impact of high-energy ions on thin films deposited by ALD is still largely unexplored. Since ALD is a different deposition method during which the sample is alternately exposed to the precursor and the plasma, it is interesting to study the influence of substrate biasing specifically for this deposition method.

This article discusses the implementation of substrate-tuned biasing and radio frequency (RF) substrate biasing in a remote plasma ALD reactor. The impact of substrate biasing on the ion energy distribution (IED) and the plasma properties are reported, as well as the effects of substrate biasing during plasma-assisted ALD of metal-oxides. The results demonstrate that substrate biasing is a promising technique to tailor the material properties of thin films synthesized by plasma-assisted ALD.

[a)]Author to whom correspondence should be addressed; electronic mail: w.m.m.kessels@tue.nl

Downloaded 17 Oct 2012 to 131.155.151.137. Redistribution subject to AVS license or copyright; see http://avspublications.org/jvsta/about/rights_and_permissions

II. THEORETICAL ASPECTS

A. Ion-bombardment during plasma processing

Processing plasmas are typically generated by supplying AC electrical power (mostly at RF, 13.56 MHz) to a gas, which leads to the acceleration and heating of electrons. The hot electrons are able to dissociate, ionize, and excite gas-phase species during the collisions they undergo. The density of these electrons is equal to the density of ions, when looking at length scales larger than the Debye length (i.e., the screening length of the charge carriers, typically 10^{-4}–10^{-3} m for remote plasma ALD conditions) and when the presence of negative ions can be neglected. However, between the plasma and a surface, a positive space charge layer builds up because the thermal velocity of the electrons is much higher than the thermal velocity of the (much heavier) ions. The voltage across this so-called plasma sheath is such that the flux of ions and electrons is balanced by retarding electrons and accelerating ions.[3,5] This means, for example, that for a floating substrate the net electrical current to electrically floating surfaces in contact with the plasma is zero. In the case of a collisionless plasma sheath, the pressure in the reactor is sufficiently low to prevent collisions between ions and neutral gas species in the plasma sheath. Consequently, ions are accelerated over the full sheath and the ion energy, E_{ion} [expressed in eV], at the substrate surface is given by

$$E_{ion} = e \cdot V_{sheath} = e \cdot (V_{plasma} - V_{subs}), \quad (1)$$

where e is the electron charge, V_{sheath} is the voltage across the plasma sheath, V_{plasma} is the plasma potential, and V_{subs} is the substrate potential. For a grounded substrate stage (i.e., $V_{subs} = 0$ V), the sheath voltage is equal to the plasma potential. The equation furthermore illustrates that the energy of the ions can be increased by applying a voltage to the substrate stage that is, on average, negative. Usually this negative bias voltage is applied using DC, AC, RF, or more complex signals.[4,12]

B. Substrate-tuned biasing and RF biasing

Substrate-tuned biasing (or substrate-tuning) is a technique to vary the voltage across the plasma sheath at the substrate stage, without the need for an external bias source. The mechanism behind this technique is the tuning of the impedance between the substrate stage and the ground, using an external electrical circuit.[13,14] In Fig. 1, a remote plasma ALD reactor equipped with substrate-tuned biasing is shown. The electrical circuit of real and equivalent components in the setup is also drawn in this figure, which makes it possible to evaluate the substrate-tuned biasing technique electrically. In Table I, the components are summed up and described, while a more detailed description is given in this section.

The electrical power used to generate the inductively coupled plasma (ICP) plasma is provided by a RF (13.56 MHz) power supply. The power source is connected to the ICP coil through a L-type matching network with two variable capacitors C_{i1} and C_{i2}, designed to match inductive loads. The inductive coupling of the power is represented by

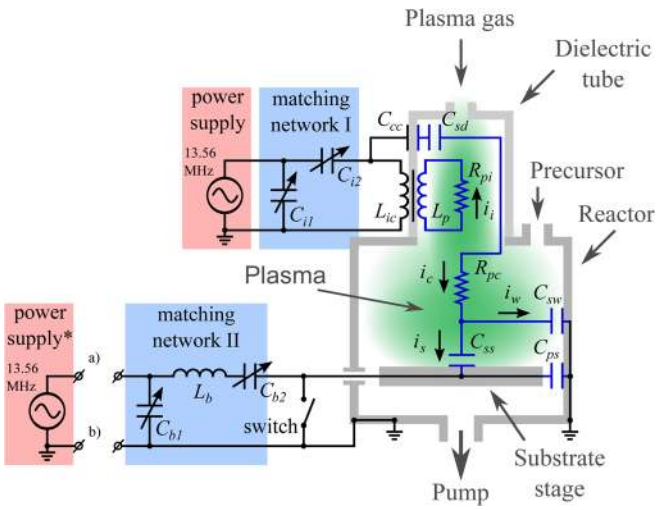

FIG. 1. (Color online) Remote plasma ALD reactor equipped with an inductively-coupled plasma source. Real electrical components are drawn in black whereas equivalent electrical components describing the plasma behavior are drawn in blue (see also Table I). A matching network is connected to the substrate stage to control the substrate potential by substrate-tuned biasing. The corresponding RF power supply can additionally be connected to the matching network at nodes "(a)" and "(b)" for RF biasing. The substrate stage can be electrically grounded by closing the switch.

a transformer, where L_{ic} is the five-turn Cu coil wrapped around the dielectric tube on top of the reactor and L_p accounts for the induced electron current, which generates the plasma. ICP sources are typically nonideal, and electrical power is also partly capacitively coupled through C_{cc}, which is the capacitance across the walls of the dielectric tube. The resistors R_{pi} and R_{pc} represent the dissipation of electrical power by the plasma, whereas C_{sd}, C_{sw}, and C_{ss} denote the plasma sheath capacitances between the plasma and the dielectric tube, the plasma and the grounded reactor wall, and the plasma and the substrate stage, respectively. Furthermore, the parasitic capacitance present between the substrate stage and the reactor walls is represented by C_{ps}. A matching network, designed to match capacitive loads using two

TABLE I. Overview of the electrical components given in the electrical circuit in Fig. 1. To distinguish real components from equivalent electrical components, the latter are marked with an asterisk.

Part of the circuit	Symbol	Component
Inductive coupling	L_{icp}	Coil inductance
	L_p	Plasma inductance*
	R_{pi}	Plasma resistance*
Capacitive coupling	C_{ccp}	Capacitance across dielectric tube*
	C_{sd}	Sheath capacitance at dielectric tube*
	C_{sw}	Sheath capacitance at wall*
	C_{ss}	Sheath capacitance at substrate*
	C_{ps}	Stray capacitance at substrate*
	R_{pc}	Plasma resistance*
Matching network I	C_{i1}	Variable parallel capacitor
	C_{i2}	Variable series capacitor
Matching network II	C_{b1}	Variable parallel capacitor
	C_{b2}	Variable series capacitor
	L_b	Series coil

Downloaded 17 Oct 2012 to 131.155.151.137. Redistribution subject to AVS license or copyright; see http://avspublications.org/jvsta/about/rights_and_permissions

variable capacitors, C_{b1} and C_{b2}, and a coil, L_b, is connected to the substrate stage to control the substrate voltage V_{subs} by substrate-tuned biasing. i_c and i_i denotes the flow of electrical RF current into the plasma as a result of capacitive and inductive coupling, whereas i_w and i_s are the RF currents toward the grounded reactor wall and the substrate stage, respectively.

The impedance of the substrate-ground branch (i.e., the current path from the plasma to the ground via the substrate stage), Z_{subs}, and the impedance to the wall, Z_{wall}, determine the RF current flow to the substrate, i_s, and the RF current flow to the wall, i_w. These currents can be expressed as

$$i_s = i_c \cdot \frac{|Z_{wall}|}{|Z_{wall}| + |Z_{subs}|} \tag{2a}$$

and

$$i_w = i_c \cdot \frac{|Z_{subs}|}{|Z_{wall}| + |Z_{subs}|}, \tag{2b}$$

where

$$Z_{subs} = jX_{subs} = \frac{\frac{-j}{\omega C_{ps}} \cdot \left(\omega L_b - \frac{1}{\omega C_b}\right)}{\omega L_b - \frac{1}{\omega C_b} - \frac{1}{\omega C_{ps}}} - \frac{j}{\omega C_{ss}} \tag{3a}$$

and

$$Z_{wall} = jX_{wall} = \frac{-j}{\omega C_{sw}}. \tag{3b}$$

X_{subs} is the reactance of the substrate-ground branch, i.e., the imaginary part of Z_{subs}, and C_b is assumed $C_{b1} + C_{b2}$. The higher i_s, the higher the average voltage across the plasma sheath at the substrate, $V_{ss,avg}$, will become to keep the net flux of ions and electrons to the substrate zero. For $V_{ss,avg} > V_{plasma}$, the average substrate voltage, $V_{subs,avg}$, will be negative [see Eq. (1)]. The sheath capacitance at the substrate, C_{ss}, can be expressed as[14,15]

$$C_{ss} = \frac{dQ_{ss}}{dV_{ss}} = Aen_e \frac{dt_{ss}}{dV_{ss}} = \frac{0.76A\sqrt{\varepsilon_0 n_e e}}{(T_e V_{ss})^{1/4}}, \tag{4}$$

where Q_{ss} is the charge in the plasma sheath at the substrate, A is the substrate stage area, t_{ss} is the sheath thickness at the substrate, ε_0 is the vacuum permittivity, n_e is the electron density, k is the Boltzmann constant, and T_e is the electron temperature [expressed in (eV)].

The impedance of the substrate-ground branch, Z_{subs}, can be tuned by varying C_b. For relatively low values of C_b, the value of Z_{subs} is negative (i.e., the impedance is capacitive). An increase of C_b will decrease Z_{subs} (i.e., less negative) and increase i_s. Consequently, V_{ss} will increase in order to balance the fluxes of ions and electrons to the substrate stage. According to Eq. (4), an increase of V_{ss} will decrease C_{ss} (assuming that n_e and T_e remain relatively constant) and Z_{subs} will then increase (i.e., more negative), thereby stabilizing V_{ss}. Therefore, V_{ss} can be controlled continuously by varying C_b, as long as Z_{subs} is negative (i.e., for every value of C_b there is a V_{ss}). V_{ss} is at its maximum when $Z_{subs} = 0\ \Omega$, which is when the substrate-ground branch is in series resonance. For values of C_b higher than for the resonance condition, Z_{subs} is positive (i.e., the impedance is inductive). An increase of C_b will increase Z_{subs} (i.e., more positive), V_{ss} will decrease and C_{ss} will increase. Because an increase in C_{ss} will increase Z_{subs} (i.e., more positive) even more, no stable situation will be reached and Z_{subs} will keep increasing. i_s will become low and, consequently, V_{ss} will also be low.

In order to allow for the use of the substrate-tuned biasing technique, the components and variables in Eqs. (4a) and (4b) should have values such that Z_{subs} can be tuned to values (significantly) lower than Z_{wall}. If, for example, the substrate stage area, A, is too large, then C_{ss} is too large and Z_{subs} is positive (i.e., the impedance is inductive) for the full tunable range of C_b and, consequently, V_{ss} cannot be controlled. In this situation, or when the maximum V_{ss} obtainable by substrate-tuned biasing is not sufficient for a specific application, an external RF power source can be used. This power source is connected to nodes (a) and (b) in Fig. 1. By supplying RF power to the substrate, i_s can be controlled and, as a result, V_{ss} can be increased. RF biasing is addressed extensively in the literature, for example, the reader is referred to Refs. 3–5.

III. EXPERIMENT

A. Plasma-assisted ALD reactor

All experiments were carried out in the home-built remote plasma ALD reactor, as schematically illustrated in Fig. 1.[16] The ICP source mounted on top of the reactor was used to generate plasmas in gases such as Ar, H_2, N_2, O_2, and NH_3, which were supplied via the dielectric tube. The base pressure of the system was $\sim 10^{-6}$ Torr, which was achieved by using a rotary vane pump and a maglev turbo molecular pump. Typical values for the gas pressure and the ICP power were 7.5 mTorr and 200 W, respectively. For some of the experiments reported in this article, however, ICP powers up to 550 W were used, during which the ICP coil was cooled by an additional air flow. The substrate temperature was monitored by a thermocouple connected to the substrate stage and controllable up to 400 °C by a proportional-integral-differential controller (PID controller). The temperature of the reactor walls (typically 80 °C), the precursor containers (up to 100 °C, depending on the precursor), and the corresponding precursor lines (typically 15 °C higher than the precursor container, to prevent precursor condensation in the lines) were individually controlled by temperature regulators. The system hardware was operated using a National Instruments compact Fieldpoint programmable automation controller and in-house developed LabVIEW software.

B. Substrate-tuned biasing and RF biasing

In order to have the possibility to apply a bias voltage to it, the substrate stage was electrically isolated from the grounded reactor wall using ceramic insulators. A flange with two electrical feed-throughs was connected to the reactor, where one

Downloaded 17 Oct 2012 to 131.155.151.137. Redistribution subject to AVS license or copyright; see http://avspublications.org/jvsta/about/rights_and_permissions

was connected to a *L*-type matching network, whereas the other was connected to an oscilloscope via a 100:1 probe to measure the substrate bias voltage. During the experiments, C_{b1} and L_b, present in the matching network, were kept constant at 136 ± 7 pF and 1.5 ± 0.1 μH, whereas C_{b2} was varied between 173 ± 9 and 932 ± 47 pF. The capacitances and self-inductance were measured using a LC-meter. It was furthermore possible to electrically ground the substrate stage through a switch.

During plasma exposure with substrate-tuned biasing or RF biasing enabled, the power supply to the resistive heating element integrated in the substrate stage was temporarily disabled by a relays. This was essential, as the additional impedance from the power source of the heater prevented the use of the substrate-tuned biasing technique for high substrate bias voltages. Since relatively short plasma exposures are usually required during the ALD deposition process (several seconds at maximum, which is typically $\leq$25% of the cycle time), the substrate temperature was hardly affected by temporarily disabling the substrate heating. The latter was also facilitated by the well-calibrated PID temperature controller.

A home-built double Langmuir probe with Pt tips was aligned at approximately 1 cm above the substrate stage to measure *IV*-curves from which the electron temperature, T_e, and the electron density, n_e, were calculated using the method described by Peterson and Talbot.[17] The signal was filtered by a LC electrical network to remove unwanted RF components. For the ion energy and ion flux measurements, an Impedans Semion retarding field energy analyzer (RFEA) was employed, placed on the substrate stage.[18] Optical emission measurements were performed using an OceanOptics UBS4000-UV-VIS spectrometer (200–850 nm wavelength range) through a quartz window, aligned at approximately 1 cm above the substrate stage.[19] It is noted that it was verified that the plasma did not significantly heat the samples during the deposition process using a thermocouple connected to the substrate stage.

C. Thin film deposition and characterization

The effects of substrate-tuned biasing and RF substrate biasing were evaluated for Al_2O_3, Co_3O_4, and TiO_2 thin films deposited by plasma-assisted ALD. In the case of a grounded substrate, the switch in Fig. 1 was closed. Substrate-tuned biasing was used for bias voltages of -50 and -100 V and RF biasing was employed for -150 and -200 V (see Sec. IV A for more details on these choices). During the plasma exposure step, the power supply to the substrate heater was switched off, to allow for a substrate bias signal to be applied to the substrate stage (see Sec. III B). During deposition of the metal-oxide films, O_2 [>99.999% purity] was provided through the quartz tube continuously, as none of the precursors showed a reaction with O_2 gas at the conditions employed. The operating pressure was 7.5 mTorr and 200 W ICP power was supplied during the second half-cycle of the deposition process. Unless noted otherwise, 1×1 in. substrates with $\sim$2 nm native oxide cut from *n*-type c-Si (100) wafers with resistivity 10–20 Ω cm have been used.

For the deposition of Al_2O_3, trimethylaluminium [$AlMe_3$, purity 99.99%, purchased from Akzo Nobel] was used as the precursor.[20] The precursor container was not heated and no Ar bubbling was required, as the vapor pressure of $AlMe_3$ was sufficiently high at room temperature. The precursor dose time, precursor purge time, plasma dose time, and plasma purge time were set to 50 ms, 3 s, 2 s, and 3 s, respectively. Al_2O_3 films of approximately 25 nm thick were deposited at 25 and 200 °C. The Co_3O_4 films were deposited from cobaltocene [$CoCp_2$, purity 98%, purchased from Strem Chemicals] as the precursor, kept in a precursor container that was heated to 80 °C. Additionally, Ar bubbling [>99.999% purity] was used.[21] During processing, the dose and purge times were 2, 5, 5, and 5 s, respectively. Co_3O_4 films of approximately 25 nm thick were deposited at 300 °C. For the deposition of the TiO_2 films, Star-Ti [$Ti(Cp^{Me5})(OMe)_3$, purity >99%, donated by Air Liquide] was used as the precursor.[22] The bubbler was heated to 78 °C, and Ar bubbling was used. During processing, all dose and purge times were set to 5 s. TiO_2 films of approximately 30 nm thick were deposited at 300 °C.

Several techniques were used for the characterization of the thin films properties. The film thickness was measured *ex situ* by spectroscopic ellipsometry (SE) using a J.A. Woollam M2000D rotating compensator ellipsometer and CompleteEASE software. As proposed by Langereis *et al.*, a Cauchy oscillator was used for the optical model of Al_2O_3, whereas two Tauc-Lorentz oscillators were used to parameterize TiO_2.[23] For the optical model of the Co_3O_4 films, a combination of a Gauss, a Tauc–Lorentz, and two Lorentz oscillators was used, as reported by Donders *et al.*[21] The mass density and the crystallinity of the films were determined by x-ray reflectometry (XRR) and grazing-incidence x-ray diffraction (GI-XRD), respectively. For both techniques, PANalytical's X'Pert PRO MRD system was used. The composition of the Al_2O_3 and Co_3O_4 films was studied by x-ray photoelectron spectroscopy (XPS) using a Thermo Scientific K-Alpha KA1066 spectrometer. Additionally, wafer-curvature tests were carried out at room temperature with a kSA MOS Ultra-Scan system to determine the curvature of 4 in. wafers before and after deposition of the Al_2O_3 films. From the difference in curvature, the stress of the Al_2O_3 films was calculated using the Stoney equation.[24]

IV. RESULTS

A. Substrate-tuned biasing and RF biasing

In Fig. 2(a), the substrate-tuned bias voltage, V_{subs}, is displayed as a function of time, and in Fig. 2(b), the corresponding IEDs are shown. The voltage waveforms were measured by an oscilloscope for various settings of C_{b2}. The frequency of the voltage signals is 13.56 MHz, which is equal to the frequency applied to the ICP source. Also the voltage signal for which the substrate stage was electrically grounded (i.e., the switch in Fig. 1 is closed and $V_{subs} = 0$ V) is included. In all cases, the average substrate voltage, $V_{subs,avg}$, (also referred to as the DC-self bias voltage) is negative and has a value for which the net flux of ions and electrons to the substrate stage is zero within one RF cycle. Most of the time, the substrate voltage is negative, and ions are accelerated toward the substrate stage. During a short fraction of the

Downloaded 17 Oct 2012 to 131.155.151.137. Redistribution subject to AVS license or copyright; see http://avspublications.org/jvsta/about/rights_and_permissions

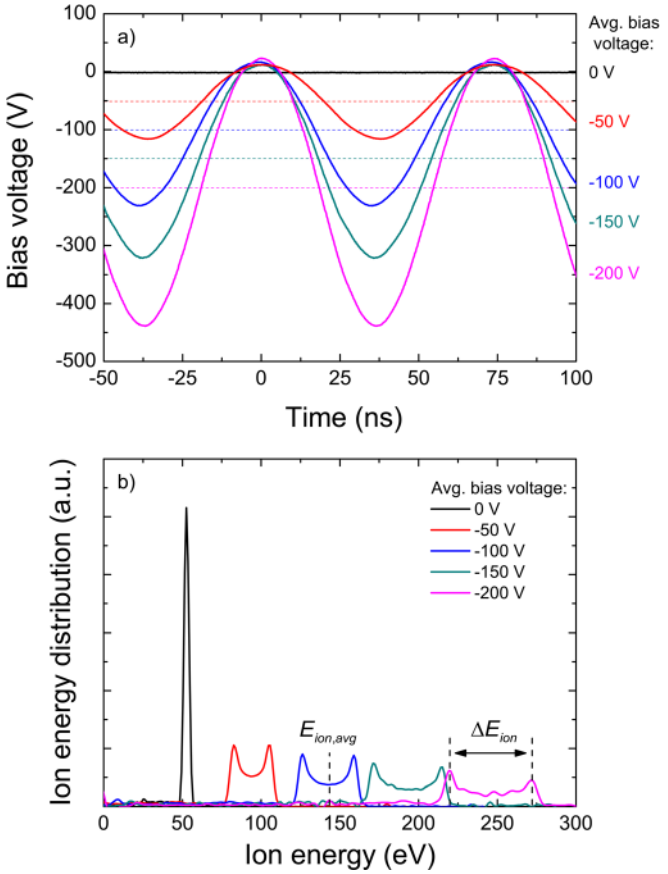

FIG. 2. (Color online) (a) Substrate-tuned bias voltage as a function of time and (b) corresponding IEDs. The plasmas were generated in O_2 at 550 W ICP power and 7.5 mTorr pressure. Data are given for substrate-tuned bias voltages of 0 to −200 V, obtained by varying C_{b2} in the matching network connected to the substrate stage. The average bias voltages are also displayed with the curves, to link the voltage waveforms in (a) with the IEDs in (b). The average ion energy, $E_{ion,avg}$, and the ion energy distribution width, ΔE_{ion}, are indicated. It is noted that the phase of the voltage-signals also varies with the substrate-ground impedance. The information about the phase is, however, not visible in the graph since signal-triggering was used on the oscilloscope.

RF cycle, however, the bias signal approaches the positive plasma potential, and a flux of electrons is incident on the substrate. The IEDs demonstrate that the ion energy increases when the bias voltage is increased. When the substrate stage is electrically grounded, the IED is monomodal and $E_{ion} = 53 \pm 1$ eV, from which it can be deduced that V_{plasma} is 53 ± 1 V. When a substrate-tuned bias voltage is applied, the ion energy distribution becomes bimodal. The average ion energy, $E_{ion,avg}$, remains approximately equal to $e{\cdot}(V_{plasma} - V_{subs,avg})$, which indicates that V_{plasma} stays relatively constant [see also Eq. (1)]. When a substrate-tuned bias voltage is applied, the ion energy distribution width, ΔE_{ion}, increases as the ion transit time through the plasma sheath is smaller than the RF cycle time.[3–5] Consequently, the ions respond to the voltage across the sheath at the instant they pass the sheath, and for that reason, some ions obtain more energy than others, resulting in a bimodal IED. When a substrate-tuned bias voltage of −200 V is applied, $E_{ion,avg}$ is 246 ± 1 eV and ΔE_{ion} is 52 ± 1 eV, with minimal and maximum energies of 219 ± 1 and 272 ± 1 eV, respectively. The ion flux has been determined from the ion current measured by the RFEA and its value is $(1.7 \pm 0.1) \cdot 10^{14}\,\mathrm{cm}^{-2}\,\mathrm{s}^{-1}$ for a grounded substrate stage, whereas it decreases slightly to $(1.0 \pm 0.1) \cdot 10^{14}\,\mathrm{cm}^{-2}\,\mathrm{s}^{-1}$ for an average bias voltage of −200 V.

Data illustrating the relation between $V_{subs,avg}$ and C_{b2} are shown in Fig. 3(a), obtained by gradually increasing C_{b2} from its minimum to its maximum value for different ICP powers. For values of C_{b2} lower than a certain threshold value, $V_{subs,avg}$ increases in magnitude (i.e., its value becomes more negative) with increasing C_{b2}. The impedance of the substrate-ground branch is negative, and consequently, there belongs a $V_{subs,avg}$ for every value of C_{b2}, as long as C_{b2} stays below the threshold value (see Sec. II B). For values of C_{b2} higher than the threshold value, $V_{subs,avg}$ decreases rapidly in magnitude and eventually becomes positive when the impedance of the substrate-ground branch has become relatively high. The maximum attainable $V_{subs,avg}$ increases with increasing ICP power as a result of enhanced capacitive coupling of power into the plasma at higher powers (i.e., i_c in Fig. 1 increases).[14] The threshold value for C_{b2} is affected by the ICP power as well, because the substrate sheath capacitance, C_{ss}, is a function of n_e [see Eq. (4)]. Although not shown, it is noteworthy that the maximum $V_{subs,avg}$ will be found for a different C_{b2}, when the capacitor value is decreased from its maximum value to its minimum value. This is due to the nonlinear behavior of the substrate-ground branch with respect to variations in V_{ss}, T_e, and n_e.

IEDs have also been measured for plasmas generated in Ar, O_2, N_2, and H_2 for substrate-tuned bias voltages of −25 and −50 V, at an ICP power of 200 W and a gas pressure 7.5 mTorr. According to the literature, the dominant ions in plasmas operated under the present conditions are Ar^+, O_2^+, N_2^+, and H_3^+, respectively.[24–26] For each IED, ΔE_{ion} is derived and plotted in Fig. 4 against the root of the reciprocal ion mass. ΔE_{ion} is higher for ions with a lower mass, because these ions have a higher velocity and therefore a lower ion transit time. Although ΔE_{ion} is also affected by possible variations in T_e and n_e with changing plasma gases, such

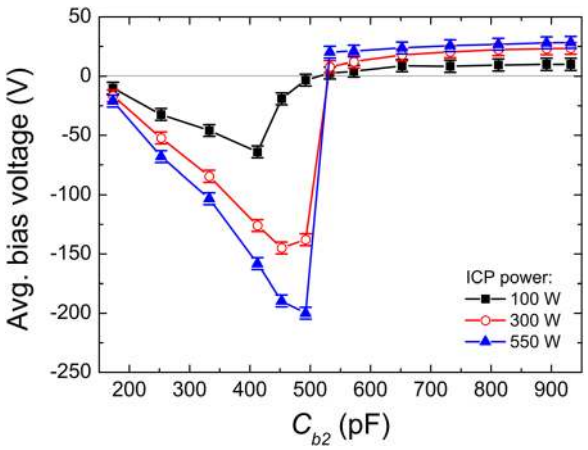

FIG. 3. (Color online) Average substrate-tuned bias voltage as a function of C_{b2}, given for different ICP powers. The plasmas were generated in O_2 at a pressure 7.5 mTorr. The maximum substrate-tuned bias voltage for a given power is obtained when the substrate-branch is in resonance.

Downloaded 17 Oct 2012 to 131.155.151.137. Redistribution subject to AVS license or copyright; see http://avspublications.org/jvsta/about/rights_and_permissions

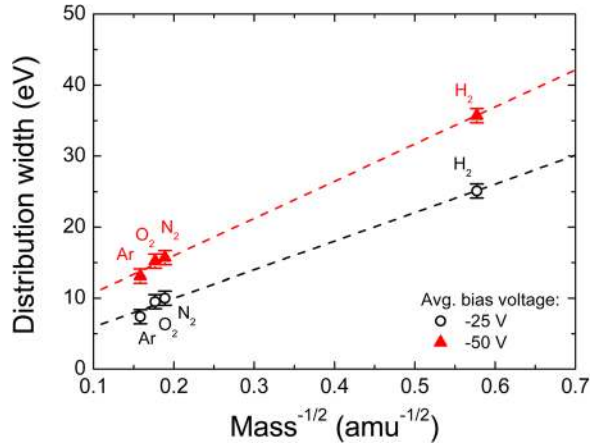

FIG. 4. (Color online) Ion energy distribution width ΔE_{ion} vs the square root of the reciprocal mass of the dominant ions in the plasma. Datapoints are given for different plasmas and substrate-tuned bias voltages of −25 and −50 V. The plasmas were generated at an ICP power of 200 W and a pressure 7.5 mTorr. The data points were fitted linearly.

variations are probably minor as the data points can be fitted well by a linear curve[5] for each bias voltage.

The influence of substrate-tuned biasing on the electron temperature T_e and the electron density n_e has also been investigated. Plots illustrating the relation between $V_{subs,avg}$ and T_e and n_e are shown in Figs. 5(a) and 5(b). For a grounded substrate stage, T_e is 2.9 ± 1.0 eV and n_e is $(2.6 \pm 0.5) \cdot 10^9$ cm^{-3} at 100 W ICP power. Data are also given for higher ICP powers. Evidently T_e is hardly influenced by the power, whereas n_e increases to $(4.6 \pm 0.9) \cdot 10^9$ cm^{-3} when the power is increased to 550 W, as expected for inductively coupled plasmas.[3] When the substrate-tuned bias voltage is increased, T_e increases from 2.9 ± 1.0 eV at 0 V to 5.9 ± 1.0 eV at −200 V, when the power is 550 W. The increasing value of T_e indicates that the plasma becomes more ionizing at the substrate level as a result of enhanced capacitive coupling. The electron density is affected by the substrate-tuned bias voltage as well, as it decreases from $(4.6 \pm 0.9) \cdot 10^9$ cm^{-3} at 0 V to $(1.4 \pm 0.3) \cdot 10^9$ cm^{-3} for −200 V, at a plasma power of 550 W. The decrease in the ion density can explain for the decrease in the ion flux with increasing bias voltage.

Also the plasma emission has been monitored. The integrated optical emission spectrum (200–850 nm range) is plotted against the substrate-tuned bias voltage in Fig. 6. Data are given for different ICP powers, and as illustrated, the integrated optical emission intensity increases with increasing ICP power. This originates from an increase in n_e with the ICP power, resulting in a higher number of electron-induced excitation reactions. The optical emission intensity also increases with V_{subs}, despite the fact that n_e showed to decrease with V_{subs} in Fig. 5(b). The emission intensity is enhanced because the excitation rate of the atoms and molecules in the plasma is highly affected by T_e [as shown in Fig. 5(a)], which increases with V_{subs}. The increase in emission intensity as a function of the ICP power and the bias voltage can also be confirmed by observations made by the naked eye, as exemplified in the photograph in the inset of Fig. 6. An increased emission intensity around the substrate stage for increased bias voltages has also been reported by Smets *et al.* in a remote expanding thermal plasma (ETP) setup used for plasma-enhanced CVD of a-Si:H.[27]

As discussed in Sec. II B, RF biasing can be used to obtain higher substrate bias voltages than achievable with substrate-tuned biasing only. In Fig. 7, $V_{subs,avg}$ is plotted as a function of the RF bias power for both the substrate-tuned biasing and the RF biasing techniques. The plasma is generated in O_2 employing an ICP power of 200 W and an O_2 pressure of 7.5 mTorr. As shown, the maximum obtainable $V_{subs,avg}$ with substrate-tuned biasing for this ICP power is −116 V. With the RF bias source connected to the matching network, the maximum attainable substrate-tuned bias voltage decreases to −75 V. This is a result of a change in the

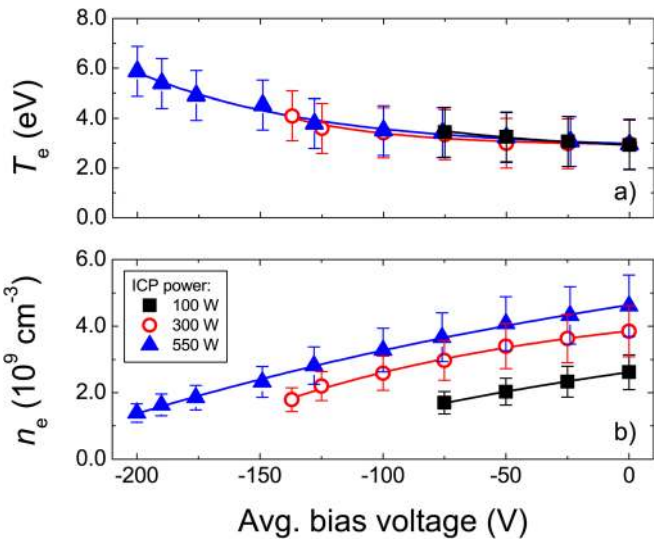

FIG. 5. (Color online) (a) Electron temperature, T_e, and (b) electron density, n_e, as a function of the average substrate-tuned bias voltage. The plasmas were generated in O_2 at 7.5 mTorr pressure and 100–550 W ICP power. Lines serve as a guide to the eye.

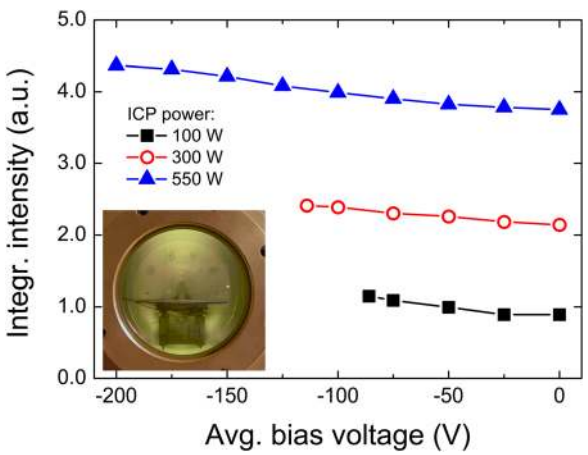

FIG. 6. (Color online) Integrated optical emission intensity (200–850 nm) provided for different substrate-tuned bias voltages. The plasmas were generated in O_2 at 100–550 W ICP power and 7.5 mTorr pressure. The optical emission was recorded directly above the substrate stage. The inset shows the substrate stage in the remote plasma ALD reactor, surrounded by the characteristic green glow of an O_2 plasma.

Downloaded 17 Oct 2012 to 131.155.151.137. Redistribution subject to AVS license or copyright; see http://avspublications.org/jvsta/about/rights_and_permissions

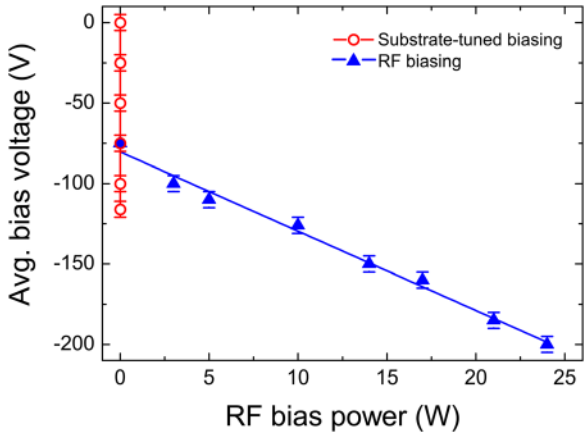

FIG. 7. (Color online) Graph showing the range of average substrate bias voltages that were achieved when substrate-tuned biasing or RF biasing was used for an ICP power of 200 W. The plasmas were generated in O_2 at 7.5 mTorr pressure. A RF power supply was additionally connected in the case of RF biasing to supply 0–24 W bias power to the substrate stage. Lines serve as a guide to the eye.

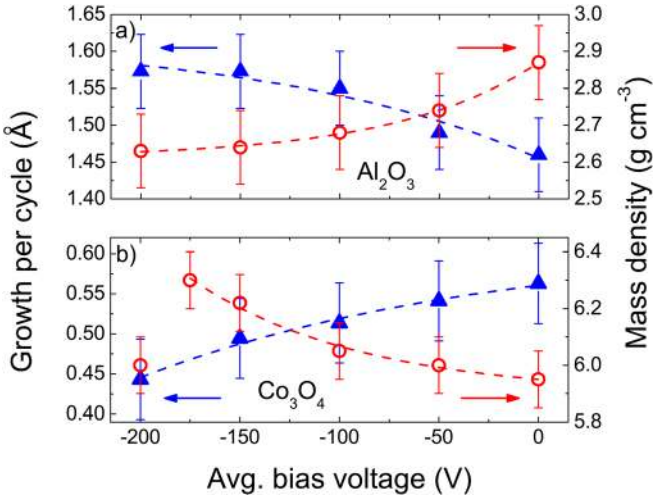

FIG. 8. (Color online) Growth per cycle and mass density of (a) Al_2O_3 films and (b) Co_3O_4 films deposited with bias voltages ranging from 0 to −200 V. Substrate-tuned biasing was employed for 0 to −100 V, whereas 0–24 W RF substrate biasing was applied for −150 and −200 V. Lines serve as a guide to the eye.

impedance of the substrate-branch. When the bias power source is switched on and C_{b1} and C_{b2} are properly adjusted, V_{subs} can be increased. An average RF bias voltage of −200 V is obtained for a bias power of 24 W. The resulting substrate voltage signals and ion energy distributions are comparable to those measured for substrate-tuned biasing [see Figs. 2(a) and 2(b)].

B. Effects of substrate biasing on metal-oxide thin film growth

1. Al_2O_3 films

In Fig. 8(a), the growth per cycle (GPC) and mass density of the films are shown as a function of the average bias voltage. For a substrate bias voltage of 0 V, the GPC is 1.46 ± 0.05 Å, and the film density is 2.9 ± 0.1 g · cm^{-3}. The growth per cycle increases to 1.55 ± 0.05 Å and 1.57 ± 0.05 Å for bias voltages of −100 and −200 V, respectively. The mass density, however, shows a decreasing trend with increasing bias voltage, which might explain for the increased growth rate. At −100 V bias voltage, the mass density is 2.7 ± 0.1 g · cm^{-3}, and at −200 V, the mass density has decreased to 2.6 ± 0.1 g · cm^{-3}. According to the compositional data obtained by XPS, the film that has been deposited at 0 V is virtually stoichiometric with an [O]/[Al] ratio of 1.51 ± 0.05 and no observable amount of C in the bulk. For substrate bias voltages of −100 and −200 V, the [O]/[Al] ratio increases to 1.55 ± 0.05 and 1.56 ± 0.05, respectively, as a result of excess hydroxyl groups into the films. Furthermore, a C content of 0.5 at. % has been measured for the film deposited at −100 V, whereas the C content is 0.6 at. % for the film deposited at −200 V. The C incorporated in the films is expected to originate from the methyl ligands in the precursor which have been decomposed by the impact of high-energy ions from the plasma. The Al_2O_3 films are amorphous for the full range of bias voltages employed.

Figure 9 shows the residual stress of the Al_2O_3 films on the Si substrates for substrate temperatures of 25 and 200 °C. In the absence of a substrate bias voltage, a residual stress of −630 ± 25 MPa has been found for the film deposited at 25 °C, whereas 153 ± 25 MPa has been found for 200 °C. The stress in the Al_2O_3 is compressive for 25 °C and most likely induced by the ions from the plasma.[9] For the film deposited at 200 °C, however, a tensile residual stress has been measured which agrees with the results reported by Puurunen *et al.* for Al_2O_3 films deposited by thermal ALD.[28] The tensile stress most likely originates from the difference in thermal expansion coefficients of the Si substrate and the Al_2O_3 film,[29,30] however, the stress might also be partly present in the Al_2O_3 layer itself. When the substrate bias voltage is increased, the stress in the film deposited at 200 °C becomes compressive and the stress values become comparable to what has been measured for the film deposited at 25 °C. This might indicate that the impact of ions on the film stress has become stronger than the effect of the elevated substrate temperature. The magnitude of the compressive stress

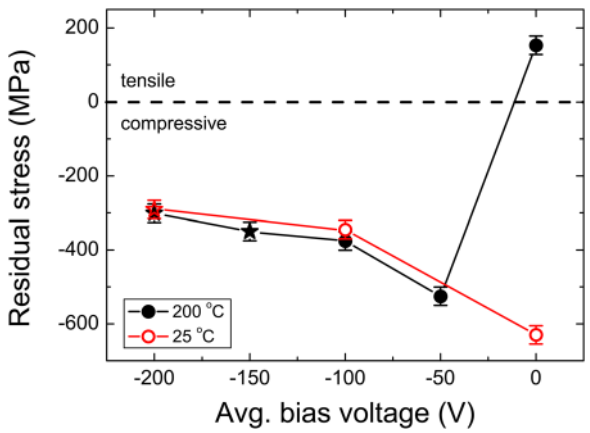

FIG. 9. (Color online) Residual film stress as a function of the average bias voltage for Al_2O_3 films deposited at 25 and 200 °C. Substrate-tuned biasing was employed for 0 to −100 V (circles), whereas 14 and 24 RF substrate biasing was applied to obtain substrate bias voltages of −150 and −200 V (stars).

Downloaded 17 Oct 2012 to 131.155.151.137. Redistribution subject to AVS license or copyright; see http://avspublications.org/jvsta/about/rights_and_permissions

decreases with increasing bias voltage for both deposition temperatures, probably because the stress relaxes as a result of the reduced film density. At −200 V, residual stress values of −291 ± 25 MPa and −301 ± 25 MPa have been found for the films deposited at 25 and 200 °C, respectively.

Nonstoichiometric Al_2O_3 films with a reduced mass density are probably of limited interest, as generally high quality dielectric films are required. The fact that the stress in the films allows to be tailored from tensile to compressive, however, may be of interest for applications in the mechanical domain or when the films serve as protective layers.

2. Co_3O_4 films

The GPC and mass density of the Co_3O_4 films are illustrated in Fig. 8(b) and show a different trend than for Al_2O_3. When the bias voltage increases, the GPC decreases while the mass density increases. Only the data point for the mass density obtained for −200 V deviates from this trend. For a grounded substrate stage, the GPC and mass density were found to be 0.56 ± 0.05 Å and 6.0 ± 0.1 g cm^{-3}, respectively, which agrees well with the values reported by Donders *et al.*[20] When the bias voltage is increased to −100 V, the growth per cycle decreases to 0.51 ± 0.05 Å and the film density increases to 6.1 ± 0.1 g·cm^{-3}. At a bias voltage of −175 V, the mass density of the films has been found to be 6.3 ± 0.1 g cm^{-3}, which is the highest value found within the range of bias voltages. For −200 V, the growth per cycle further decreases to 0.44 ± 0.05 Å, however, the mass density for this film does not fit the trend and drops to 6.0 ± 0.1 g cm^{-3}, which is approximately equal to the case with a grounded substrate. For the film that has been deposited at −200 V, it is hypothesized that the impact of high-energy ions has led to removal of material by sputtering, which might explain for the reduced mass density. Stoichiometric Co_3O_4 films with no detectable amount of C were obtained for a grounded substrate stage. The films deposited at −100 and −200 V, however, are slightly oxygen-deficient ([O]/[Co] ratio = 1.25 ± 0.05 for both samples), while no C has been observed. The Co_3O_4 films are polycrystalline for every substrate bias voltage. For more details on the GI-XRD results, the reader is referred to Ref. 21.

For many materials, the electrical, mechanical, optical, or catalytic properties improve when the mass density is higher. Therefore, these results reveal that substrate-biasing may be of interest for many more materials than Co_3O_4.

3. TiO_2 films

For TiO_2, a GPC of 0.41 ± 0.05 Å has been measured for the films deposited without a substrate bias, which is ∼24% lower than the GPC reported by Langereis *et al.*[21] The GPC increases for an increasing bias voltage and at −100 and −200 V, GPCs of 0.45 Å and 0.57 Å are obtained. In Fig. 10, XRD spectra are shown for TiO_2 films deposited with average bias voltages of 0, −100 and −200 V. In the absence of substrate biasing, the XRD spectrum shows the (101), (004), (200), (105), and (211) diffraction peaks which belong to anatase TiO_2. When the bias voltage is increased, however, most peaks corresponding to the anatase phase disappear and two new diffraction peaks, i.e., (110) and (211), appear in the spectrum which correspond to the rutile phase. At −200 V, the anatase peaks have disappeared, and only peaks corresponding to the rutile phase are visible. The change in the crystalline phase with a variation in the bias voltage was also previously reported for TiO_2 deposited in the same remote plasma ALD reactor using $Ti(Cp^{Me})(NMe_2)_3$ and O_2 plasma.[10] That study also showed that the film density decreased with ∼10% as a result of the impact of high-energy ions, an effect that is also expected to be (partly) responsible for the higher GPC observed in this study.

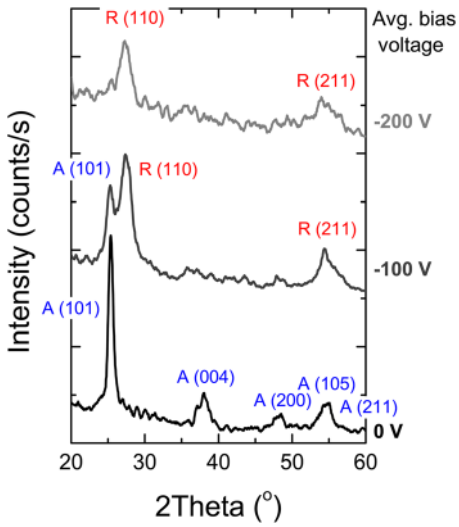

FIG. 10. (Color online) X-ray diffraction spectra for TiO_2 films deposited with bias voltages ranging from 0 to −200 V. Substrate-tuned biasing was employed for 0 to −100 V, whereas 24 W RF substrate biasing was applied for to obtain a substrate bias voltage of −200 V. Peaks corresponding to the anatase and rutile crystalline phases are denoted with "A" and "R," respectively.

The results reported for TiO_2 show that it is possible to obtain the rutile phase of TiO_2 at 300 °C, whereas usually amorphous or anatase TiO_2 is obtained unless specific starting layers or postdeposition annealing is employed.

V. CONCLUSIONS

Substrate-tuned biasing and RF biasing have been implemented in a remote plasma reactor to control the ion energy during thin film deposition by plasma-assisted ALD. Using the substrate-tuned biasing technique, the impedance between the substrate stage and the ground has been tuned and, consequently, the substrate bias voltage could be controlled. With the RF substrate biasing technique, an additional power source is connected to the substrate stage via a matching network to control the voltage at the substrate stage. The maximum average substrate-tuned bias voltage has been shown to scale with the ICP power and is −125 V for 200 W and −200 V for 550 W. When the average substrate bias voltage is −200 V, the maximum ion energy is 272 eV. The influence of substrate-tuned biasing on the electron density, the electron temperature, and the optical emission of the plasma has been studied. Alternatively, for

Downloaded 17 Oct 2012 to 131.155.151.137. Redistribution subject to AVS license or copyright; see http://avspublications.org/jvsta/about/rights_and_permissions

RF biasing at 24 W with 200 W ICP power the ion energy has been increased up to 272 eV.

The effects of substrate biasing on the material properties have been demonstrated for Al_2O_3, Co_3O_4, and TiO_2 deposited by plasma-assisted ALD. The ion-induced effects have turned out to be material and/or process-specific. For Al_2O_3, it has been found that the growth per cycle increased while the mass density decreased with higher bias voltages. This effect is expected to originate from increased incorporation of OH groups and C impurities into the films. It has also been shown that the residual stress of Al_2O_3 films on Si can be tailored from the tensile to the compressive regime by controlling the substrate bias voltage. For Co_3O_4, the growth per cycle decreases and the film density increases for higher bias voltages, as the films become slightly oxygen-deficient. Using substrate biasing, the crystalline-phase of TiO_2 films can be tailored gradually from anatase to rutile. This effect may be of interest for a variety of applications as it is not trivial to obtain as-deposited rutile TiO_2 by (plasma-assisted) ALD.

The results reported in this article demonstrate that the material properties of thin films synthesized by plasma-assisted ALD can be tailored by enhancing the ion energy using substrate biasing. Improved control over the ion energy distribution may, however, be beneficial to tailor ion-induced effects even more precisely. Bias signals that result in narrower ion energy distributions, e.g., those with higher frequencies or pulsed signals are of interest. Alternatively, the bias signal can be ramped up or down, and the timing can be varied such that substrate biasing is only enabled during part of a plasma exposure step or only during every couple of cycles. It can finally also be of interest to decouple the physical and chemical effects of the plasma exposure step, for example, by first exposing the sample to a reactive plasma (e.g., O_2 plasma) with substrate biasing disabled and subsequently to a noble gas plasma with substrate biasing enabled. These are probably just a few of the many possibilities that exist to gain more control over the ALD process and the film properties obtained.

ACKNOWLEDGMENTS

Dr. T. Fernández Landaluce, W. Keuning, J. J. A. Zeebregts, M. J. F. van de Sande, J. J. L. M. Meulendijks, C. A. A. van Helvoirt, and H. M. M. de Jong (all TU/e) are acknowledged for their assistance. This work was carried out within the Thin Film Nanomanufacturing (TFN) programme and was supported financially by the Dutch Technology Foundation STW.

[1]H. B. Profijt, S. E. Potts, M. C. M. van de Sanden, and W. M. M. Kessels, J. Vac. Sci. Technol. A **29**, 050801 (2011).
[2]H. B. Profijt, P. Kudlacek, M. C. M. van de Sanden, and W. M. M. Kessels, J. Electrochem. Soc. **158**, G88 (2011).
[3]M. A. Lieberman and A. J. Lichtenberg, *Principles of Plasma Discharges and Materials Processing*, 2nd ed. (John Wiley & Sons, New York, 2005).
[4]E. A. Edelberg, A. Perry, N. Benjamin, and E. S. Aydil, J. Vac. Sci. Technol. A **17**, 506 (1999).
[5]E. Kawamura, V. Vahedi, M. A. Lieberman, and C. K. Birdsall, Plasma Sources Sci. Technol. **8**, R45 (1999).
[6]Y. Lifshitz, S. R. Kasi, and J. W. Rabalais, Phys. Rev. B **41**, 10468 (1990).
[7]T. Takagi, J. Vac. Sci. Technol. A. **2**, 382 (1984).
[8]L. M. Williams and D. W. Hess, J. Vac. Sci. Technol. A **1**, 1810 (1983).
[9]C. A. Davis, Thin Solid Films **226**, 30 (1993).
[10]H. B. Profijt, M. C. M. van de Sanden, and W. M. M. Kessels, Electrochem. Solid-State Lett. **15**, G1 (2012).
[11]H. Kim, S. Woo, J. Lee, Y. Kim, J. Lee, I.-J. Choi, Y.-D. Kim, C.-W. Chung, and H. Jeon, J. Electrochem. Soc. **158**, H21 (2011).
[12]P. Kudlacek, R. F. Rumphorst, and M. C. M. van de Sanden, J. Appl. Phys. **106**, 073303 (2009).
[13]J. S. Logan, IBM J. Res. Dev. **14**, 172 (1970).
[14]Z. F. Ding, W. G. Huo, and Y. N. Wang, Plasma Sci. Technol. **6**, 2549 (2004).
[15]B. M. Oliver, R. M. Clements, and P. R. Smy, J. Appl. Phys **44**, 4511 (1973).
[16]E. Langereis, H. C. M. Knoops, A. J. M. Mackus, F. Roozeboom, M. C. M. van de Sanden, and W. M. M. Kessels, J. Appl. Phys. **102**, 083517 (2007).
[17]E. W. Peterson and L. Talbot, AIAA J. **8**, 2215 (1970).
[18]D. Gahan, B. Dolinaj, and M. B. Hopkins, Rev. Sci. Instrum. **79**, 033502 (2008).
[19]A. J. M. Mackus, S. B. S. Heil, E. Langereis, H. C. M. Knoops, M. C. M. van de Sanden, and W. M. M. Kessels, J. Vac. Sci. Technol. A **28**, 77 (2010).
[20]J. W. Lim and S. J. Yun, Jpn. J. Appl. Phys., Part 2 **42**, L663 (2003).
[21]M. E. Donders, H. C. M. Knoops, M. C. M. van de Sanden, W. M. M. Kessels, and P. H. L. Notten, J. Electrochem. Soc. **158**, G92 (2011).
[22]E. Langereis, R. Roijmans, F. Roozeboom, M. C. M. van de Sanden, and W. M. M. Kessels, J. Electrochem. Soc. **158**, G34 (2011).
[23]E. Langereis, S. B. S. Heil, H. C. M. Knoops, W. Keuning, M. C. M. van de Sanden, and W. M. M. Kessels, J. Phys. D **42**, 073001 (2009).
[24]L. B. Freund and S. Suresh, *Thin Film Materials, Stress, Defect Formation and Surface Evolution* (Cambridge University Press, Cambridge, U.K., 2004).
[25]N. Kang, F. Gaboriau, S.-G. Oh, and A. Ricard, Plasma Sources Sci. Technol. **20**, 045015 (2011).
[26]A. T. Hjartarson, E. G. Thorsteinsson, and J. T. Gudmundsson, Plasma Sources Sci. Technol. **19**, 065008 (2010).
[27]J. T. Gudmundsson, I. G. Kouznetsov, K. K. Patel, and M. A. Lieberman, J. Phys. D: Appl. Phys. **34**, 1100 (2001).
[28]A. H. M. Smets, W. M. M. Kessels, and M. C. M. van de Sanden, J. Appl. Phys. **102**, 073523 (2007).
[29]R. Puurunen, J. Saarilahti, and H. Kattelus, ECS Trans. **11**, 3 (2007).
[30]J. A. Thornton and D. W. Hoffman, Thin Solid Films **171**, 5 (1989).

Downloaded 17 Oct 2012 to 131.155.151.137. Redistribution subject to AVS license or copyright; see http://avspublications.org/jvsta/about/rights_and_permissions